Energy Advances

ROYAL SOCIETY OF CHEMISTRY

COMMUNICATION

View Article Online
View Journal | View Issue

Cite this: *Energy Adv.*, 2023, 2, 86

Received 25th August 2022,
Accepted 18th November 2022

DOI: 10.1039/d2ya00226d

rsc.li/energy-advances

n-Type thermoelectric behavior in oxyethylene surfactant/carbon nanotubes†

Shinichi Hata, *[a] Huynh Le Thu Thao,[a] Hiroki Ihara,[b] Yukou Du,[c] Yukihide Shiraishi *[a] and Naoki Toshima[d]

Oxyethylene surfactants were investigated as electron donors for thermoelectric (TE) carbon nanotubes (CNTs). The oxygen-barrier properties of the surfactant wrapping the NT surface and electron-donating effect of oxyethylene oxygen atoms enabled the preparation of n-type CNTs. The TE output of these NTs was comparable with that of conventionally used dopants.

Flexible and lightweight carbon nanotube (CNT)-based thermoelectric (TE) modules are attracting attention in a wide range of applications (*e.g.*, organic solar cells,[1] field-effect transistors,[2] wearable devices)[3] because they do not contain toxic elements and can be operated at waste heat temperatures (below 150 °C).[4–6] Research on various aspects of CNT thin films, including their thermal conductivity and thermoelectric conversion efficiency, has been conducted. However, in-plane thermal conductivity measurements of freestanding thin films made of CNTs or conductive polymers are especially difficult because of unfavorable heat flow in the films.[7,8] The conversion efficiency of CNT films can be estimated from their thermal power factor (PF):

$$\mathrm{PF} = S^2\sigma, \tag{1}$$

where S and σ are the Seebeck coefficient ($S > 0$ and $S < 0$ for p- and n-type semiconductors, respectively) and conductivity, respectively. In this regard, a bipolar structure with p- and n-type materials sandwiched between electrodes has been determined to present high thermal utilization efficiency.[9]

CNT doping has been extensively studied since its discovery in 1993.[10] However, the concept of n-type doping remains incompletely understood[11] because the electronic properties (*e.g.*, thermoelectromotive force and local density of states) of CNTs with large specific surface areas (200–1000 $m^2\ g^{-1}$)[12] are very sensitive to their chemical environment and, thus, easily switch to the p-type state. Radical anions in the graphene backbone created by electron doping (*e.g.*, ammonia,[13] alkali metals)[14] can react with electron donors, such as atmospheric oxygen, CO_2, and water.[15] Polyethylenimine has been successfully used as a Lewis-base molecular dopant; here, the lone pair of electrons on the nitrogen atom is partially injected into the NT conduction band (Fig. S1, ESI†).[16] This finding has led to investigations of other amine (*e.g.*, hydrazine,[17] diethylenetriamine,[18] naphthalene diimide,[19] reduced 1,1′-dibenzyl-4,4′-bipyridinium dichloride)[20] and phosphine (*e.g.*, 1,3-bis(diphenylphosphino)propane)[21] compounds. Considerable progress has been made in synthesizing n-type CNTs, particularly when potassium/crown ether complexes are used as doping reagents.[22] The dopant function design of cationic compounds (*e.g.*, imidazole,[23] gemini surfactant[24]) has steadily evolved; these compounds can impart long-term air stability and power generation properties. However, with a few exceptions, research remains focused on oil-soluble compounds and complex synthetic molecules that are difficult to handle owing to their toxicity and strong odor. Given disposal, reuse, and cost-effectiveness concerns and the expectation of the future widespread and long-term use of TE power sources in residential settings, the development of a new class of mild, naturally derived n-dopants characterized by high availability, biodegradability, and low toxicity is an important endeavor.[25]

Herein, we focused on candidate naturally derived electron donors containing negatively charged oxygen atoms with unshared electron pairs in their molecular structure to investigate the versatility of metal- and amine-free molecular dopants. Specifically, the dopant functions of tetraethylene glycol (EO_4) and its surfactant molecular equivalent, tetraethylene glycol monododecyl ether ($C_{12}EO_4$), are investigated (Fig. 1).

[a] *Department of Applied Chemistry, Faculty of Engineering, Sanyo-Onoda City University, Daigaku-dori, 1-1-1, Sanyo-Onoda, Yamaguchi 756-0884, Japan. E-mail: hata@rs.socu.ac.jp, shiraishi@rs.socu.ac.jp*
[b] *Graduate School of Engineering, Sanyo-Onoda City University, Daigakudo-ri, 1-1-1, Sanyo-Onoda, Yamaguchi 756-0884, Japan*
[c] *College of Chemistry, Chemical Engineering and Materials Science, Soochow University, Suzhou 215123, P. R. China*
[d] *Sanyo-Onoda City University, Daigaku-dori, 1-1-1, Sanyo-Onoda, Yamaguchi 756-0884, Japan*

† Electronic supplementary information (ESI) available. See DOI: https://doi.org/10.1039/d2ya00226d

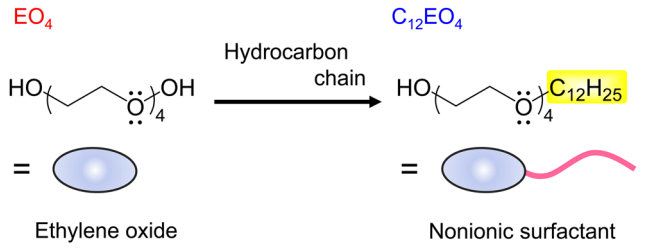

Fig. 1 Molecular structures of tetraethylene glycol (EO_4) and tetraethylene glycol monododecyl ether ($C_{12}EO_4$).

Research on oxygen-rich compounds to prepare n-type materials is limited to polyoxyethylene[26] and polyvinyl alcohol,[27] and the relationship between amphiphilic dopants and n-type CNTs remains unclear. In this study, preliminary findings on the preparation of n-type CNTs based on intermolecular electron transfer between $C_{12}EO_4$ and NTs using nonionic surfactants are presented.

Detailed information on the materials, experimental techniques, and characterization methods is provided in the ESI.† An overview of the film preparation process is shown in Fig. S2 (ESI†). The dispersion behavior and microscopic orientation of the CNT bundles in the fabricated films were observed by SEM (Fig. 2). The average diameters of pure CNT, EO_4/CNT, and $C_{12}EO_4$/CNT were estimated to be 41.8 ± 33.7, 38.0 ± 17.6, and 27.6 ± 16.1 nm, respectively. EO_4 incorporation reduced van der Waals forces and π–π interactions between CNT bundles.[28] The adsorption capacity of the films increased with the hydrocarbon chain length of the surfactant and promoted the divergence of NT bundles. $C_{12}EO_4$ weakened chemical interactions between CNTs, causing the CNT ropes to separate and form fiber bundle structures in the films. Thus, the induction of hydrophilic properties on the outer NT wall surface by adsorbed $C_{12}EO_4$ appears important for the dispersion of the CNTs in aqueous media.

The TE properties of the fabricated films (Fig. 3) were investigated in the temperature range of 330–390 K. The S values of the EO_4/CNT film at each measurement temperature ranged from 53.2 to 58.3 μV K^{-1}, and its semiconductor properties were p-type. This finding is consistent with the carrier properties of CNTs in air (S = 62.3 μV K^{-1}).[29] By contrast, the S values of the $C_{12}EO_4$/CNT film were consistently negative (range = −62.5 to −52.7 μV K^{-1}), regardless of the measurement temperature. $C_{12}EO_4$, a carrier for NTs, acts as an n-type dopant that converts the charge carriers from holes to electrons, and its σ value is higher than that of EO_4 at all measurement temperatures. This finding is supported by the SEM observations, where the increased dispersion ability of the surfactant, which features hydrocarbon chains attached to EO_4, results in finer NT bundles. The S and σ measurements showed that the PF values of $C_{12}EO_4$ were consistently superior to those of EO_4 with increasing temperature. At 363 K, the PF of $C_{12}EO_4$/CNT peaked at 214.1 μW m^{-1} K^{-2}, corresponding to an improvement of ~2.8 times compared with that of EO_4/CNT.

Fig. 4 shows the normalized spectrum of the G band associated with the vibration of the carbon atoms along the NT plane. After doping with $C_{12}EO_4$, the G band of the CNTs shifted slightly from 1589 cm^{-1} to the lower frequency region. This behavior is well observed during electron transfer from electron donors to NTs,[19] indicating that electron doping from $C_{12}EO_4$ to CNTs has occurred. The Raman D/G ratios of the pure, EO_4-doped, and $C_{12}EO_4$-doped CNTs, which indicate their crystallinity, were 0.012, 0.016, and 0.019, respectively. No significant changes in D-band intensity were observed during the doping process. In particular, no significant structural

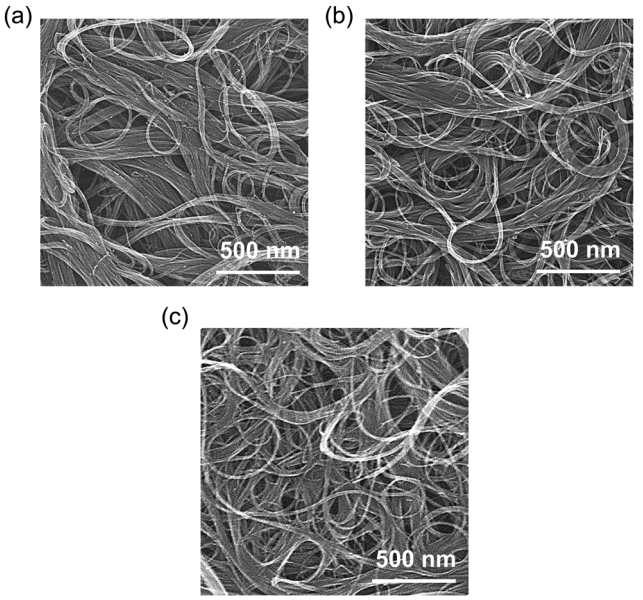

Fig. 2 SEM images of the (a) pure CNT, (b) EO_4, and (c) $C_{12}EO_4$/CNT films.

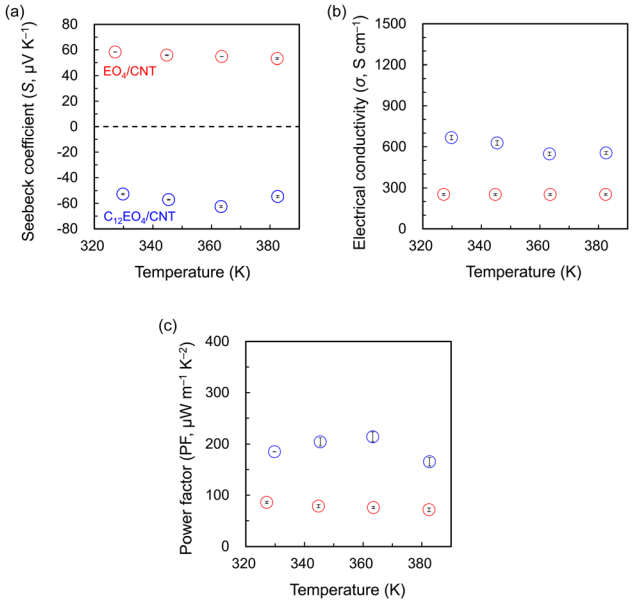

Fig. 3 Temperature dependence of the (a) Seebeck coefficient, (b) electrical conductivity, and (c) thermoelectric (TE) power factor of the TE films. Red circles, EO_4/CNT; blue circles, $C_{12}EO_4$/CNT.

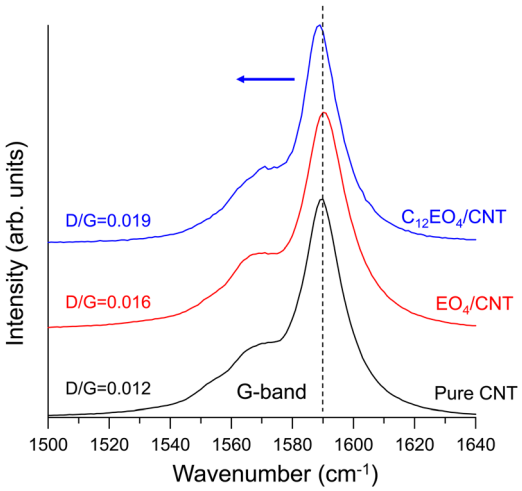

Fig. 4 Raman spectra of the pure CNT, EO_4/CNT, and $C_{12}EO_4$/CNT films.

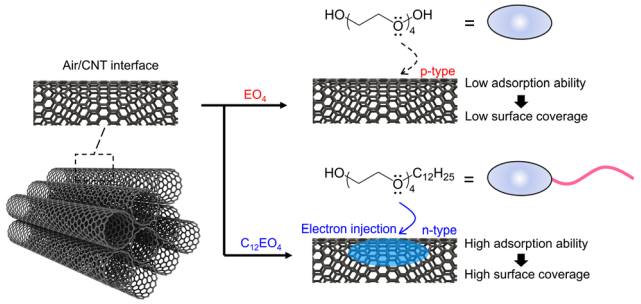

Fig. 5 Schematic diagram of electron injection associated with adsorbed $C_{12}EO_4$ on a CNT surface. Electron transfer from the dopant to the CNTs occurs with $C_{12}EO_4$ but not with EO_4. This phenomenon inhibits oxygen adsorption and facilitates electron injection from the surfactant oxyethylene unit into the CNTs. Thus, the carriers of the CNTs are converted from holes to electrons.

defects occurred after doping. These findings indicate that the noncovalent binding of $C_{12}EO_4$ to CNTs triggers electron transfer from the dopant to the CNTs. The results thus far confirm that EO_4 does not serve as an n-dopant for NTs, in contrast to $C_{12}EO_4$. In the case of EO_4, the ether oxygen in its oxyethylene group is a highly hydrophilic functional group that hydrogen-bonds with water molecules.[30] Thus, EO_4 has poor adsorption and dispersion capacities for NTs and does not effectively deband CNTs in water.

The specific surface area of bare NTs is ~56% smaller than that of pure CNTs, and most of the CNT surface is an interface accessible to molecular O_2 (Fig. S3, ESI†). The low coverage of adsorbed EO_4 could promote electrophilic reactions between molecular O_2 and the electron-activated sites of the NTs. This factor is responsible for the dominant doping of atmospheric oxygen by electron injection from the dopant into the CNTs, resulting in p-type properties, as observed in the pure CNTs. In the case of $C_{12}EO_4$, the molecule has hydrophilic and hydrophobic groups in its structure and is adsorbed on the NT wall. Its critical micelle concentration is very low at 0.06 mM,[31] which may indicate an intrinsically favorable interfacial adsorption capacity. Using TGA, we determined that the apparent amount of surfactant in the film was 23.1 wt% (Fig. S4, ESI†). The $C_{12}EO_4$ molecules weaken chemical interactions between the CNTs, causing the CNT ropes to separate and form a fiber bundle structure in the film. This highly interconnected network may play an important role in increasing the number of conduction pathways available for charge transport.[32,33] The hydrophilic groups of $C_{12}EO_4$ appear to be in contact with the NT wall; the results of systematic investigations with anionic and cationic surfactants indicate the ionic nature of the surfactant and confirm that the headgroup determines the type of charge carriers in the doped CNT.[34] In this work, the ether oxygen of the $C_{12}EO_4$ headgroup contains an isolated electron pair, which injects electrons into the CNTs during adsorption. Preliminary results obtained with the dopant polymer polyethylene glycol indicate that electrons isolated from the oxygen atom can shift the Fermi level upward and the work function downward, changing the positive S of CNTs to negative.[26] In addition, the specific surface area occupied by bare NTs is approximately 85% smaller than that of pure CNTs, and most of the CNT surface is wrapped by surfactant molecules (Fig. S3, ESI†). The adsorbed surfactant layer can conform to the curvature of the NT bundle, resulting in an irregular structure that is soft, flexible, and fluid. Such a structure provides multipoint protection around negatively charged doping sites. The number of oxygen doping sites must be considerably smaller than the number of negatively charged doping sites because the specific surface area of the bare NTs decreases as the coverage of the adsorbed surfactant increases. In such samples, molecular oxygen adsorption is inhibited, and doping with $C_{12}EO_4$ oxyethylene units render the CNT surface electron-rich, stabilizing the delocalized negative charge of n-type CNTs (Fig. 5). Recent theoretical calculations and experimental results have shown that cationic compounds (*e.g.*, imidazole,[23] gemini surfactants[24]) can tightly cover the surface of CNTs, inhibiting interaction with O_2 molecules. To test whether oxyethylene surfactants can indeed act as dispersants and dopants, nonionic surfactants with 6 or 8 mol of ethylene oxide added to dodecyl ether were studied (Fig. S5, ESI†). The doped CNTs obtained were n-type, regardless of the surfactant concentration in the aqueous solution used to disperse them in their original state. A comparison of a series of basic molecular structures indicates that oxyethylene surfactants are useful reagents capable of simultaneous carrier conversion and NT dispersion. Preliminary studies confirm that EO_4/CNTs are p-type and $C_{12}EO_4$/CNTs are n-type in the dopant concentration range of 4.3–17.0 mM in CNT dispersions (Fig. S6, ESI†). These dopant features are achieved by introducing hydrocarbons into oxyethylene, which is an important structural feature for n-dopants with a simple structure.

An atmospheric stability test of $C_{12}EO_4$/CNT was conducted to confirm carrier persistence in n-type materials (Fig. S7, ESI†). In the initial 4–5 d of the test, the S value was almost zero and the electron carriers in the CNTs were nearly deactivated. Thus, the PF value was also close to 0 even after 7 d. By contrast, when

the dopant concentration was changed from 4.3 to 17.0 mM (an increase of ~4 times), the S of $C_{12}EO_4$/CNT showed a negative value even after 7 d. Increasing the oxyethylene surfactant concentration further extended the adsorbed surfactant wrapping area on the CNT surface and appeared to inhibit n-type material degradation owing to atmospheric oxygen. This result indicates that n-type lifetimes can be improved by optimizing the dopant concentration in the film sample.

Table S1 (ESI†) summarizes the preparation and properties of the n-type CNT materials developed in this study and previous work.[7,19,21,22,26,27,35–44] With a few exceptions, the TE performance of $C_{12}EO_4$/CNTs is comparable with that of n-type films impregnated with solutions containing high concentrations of metal ions, amine compounds, and ammonium salts in organic solvents. The proposed approach is an environmentally friendly, economically feasible solution because n-type CNTs are prepared at a very low oxygen-based surfactant concentration of 4.3 mM without the need for metal ions or organic solvents. Research on converting CO_2 and biomass into organic resources of oxygen atoms through catalytic reactions is gaining momentum.[45,46] The results of this study could be adapted to contribute to a carbon-neutral society.

In summary, $C_{12}EO_4$, a surfactant with high adsorption capacity, can cover ~85% of the CNT surface, inhibiting oxygen adsorption. Electron donation from oxyethylene units to the NTs occurs simultaneously, resulting in functionalized n-type CNTs. The TE performance of the CNTs (214.1 μW m^{-1} K^{-2} at 363 K) is comparable with that of conventional CNTs incorporating nitrogen-based dopants. Further studies are needed to identify the optimal semiconductor/metal ratio of surfactant-wrapped CNT films and investigate the detailed electronic structure and carrier transport properties of the resultant materials. Such work would contribute to the future functionalization of flexible electronics.

Author contributions

S. H. and Y. S. developed the original concept and designed the experiments. S. H. wrote the manuscript. S. H. and H. L. T. T. performed the material synthesis and characterization. H. I. supported the analysis of the results. Y. D. and N. T. provided advice regarding the interpretation of the results. S. H. and Y. S. supervised the project. All authors contributed to the discussion of the results.

Conflicts of interest

The authors declare that they have no known competing financial interests or personal relationships that could have influenced the work reported in this paper.

Acknowledgements

This study was supported in part by KAKENHI projects (No. 21K14428 and 19K05633 awarded to S. H. and Y. S., respectively) from the JSPS and a Sasakawa Scientific Research Grant from The Japan Science Society, Japan.

Notes and references

1 Z. Li, V. Saini, E. Dervishi, V. P. Kunets, J. Zhang, Y. Xu, A. R. Biris, G. J. Salamo and A. S. Biris, *Appl. Phys. Lett.*, 2010, **96**, 033110.
2 A. Javey, R. Tu, D. B. Farmer, J. Guo, R. G. Gordon and H. Dai, *Nano Lett.*, 2005, **5**, 345–348.
3 Y. Zhang, Q. Zhang and G. Chen, *Carbon Energy*, 2020, **2**, 408–436.
4 J. L. Blackburn, A. J. Ferguson, C. Cho and J. C. Grunlan, *Adv. Mater.*, 2018, **30**, 1704386.
5 N. Toshima, *Synth. Met.*, 2017, **225**, 3–21.
6 C. Yu, Y. S. Kim, D. Kim and J. C. Grunlan, *Nano Lett.*, 2008, **8**, 4428–4432.
7 K. Chatterjee, A. Negi, K. Kim, J. Liu and T. K. Ghosh, *ACS Appl. Energy Mater.*, 2020, **3**, 6929–6936.
8 Z. Liang, L. Chen and G. C. Bazan, *Adv. Electron. Mater.*, 2019, **5**, 1900650.
9 Y. Sun, C. A. Di, W. Xu and D. Zhu, *Adv. Electron. Mater.*, 2019, **5**, 1800825.
10 S. Iijima and T. Ichihashi, *Nature*, 1993, **363**, 603–605.
11 V. Derycke, R. Martel, J. Appenzeller and P. Avouris, *Appl. Phys. Lett.*, 2002, **80**, 2773–2775.
12 K. Kobashi, S. Ata, T. Yamada, D. N. Futaba, T. Okazaki and K. Hata, *ACS Appl. Nano Mater.*, 2019, **2**, 4043–4047.
13 J. Kong, N. R. Franklin, C. Zhou, M. G. Chapline, S. Peng, K. Cho and H. Dai, *Science*, 2000, **287**, 622–625.
14 C. Zhou, J. Kong, E. Yenilmez and H. Dai, *Science*, 2000, **290**, 1552–1555.
15 J. T. Quinn, J. Zhu, X. Li, J. Wang and Y. Li, *J. Mater. Chem. C*, 2017, **5**, 8654–8681.
16 M. Shim, A. Javey, N. W. Shi Kam and H. Dai, *J. Am. Chem. Soc.*, 2001, **123**, 11512–11513.
17 K. S. Mistry, B. A. Larsen, J. D. Bergeson, T. M. Barnes, G. Teeter, C. Engtrakul and J. L. Blackburn, *ACS Nano*, 2011, **5**, 3714–3723.
18 G. Wu, C. Gao, G. Chen, X. Wang and H. Wang, *J. Mater. Chem. A*, 2016, **4**, 14187–14193.
19 G. Wu, Z.-G. Zhang, Y. Li, C. Gao, X. Wang and G. Chen, *ACS Nano*, 2017, **11**, 5746–5752.
20 S. M. Kim, J. H. Jang, K. K. Kim, H. K. Park, J. J. Bae, W. J. Yu, I. H. Lee, G. Kim, D. D. Loc, U. J. Kim, E.-H. Lee, H.-J. Shin, J.-Y. Choi and Y. H. Lee, *J. Am. Chem. Soc.*, 2009, **131**, 327–331.
21 Y. Nonoguchi, K. Ohashi, R. Kanazawa, K. Ashiba, K. Hata, T. Nakagawa, C. Adachi, T. Tanase and T. Kawai, *Sci. Rep.*, 2013, **3**, 3344.
22 Y. Nonoguchi, M. Nakano, T. Murayama, H. Hagino, S. Hama, K. Miyazaki, R. Matsubara, M. Nakamura and T. Kawai, *Adv. Funct. Mater.*, 2016, **26**, 3021–3028.
23 Y. Nakashima, R. Yamaguchi, F. Toshimitsu, M. Matsumoto, A. Borah, A. Staykov, M. S. Islam, S. Hayami and T. Fujigaya, *ACS Appl. Nano Mater.*, 2019, **2**, 4703–4710.

24 S. Hata, K. Maeshiro, M. Shiraishi, Y. Du, Y. Shiraishi and N. Toshima, *ACS Appl. Electron. Mater.*, 2022, **4**, 1153–1162.
25 M. Massetti, F. Jiao, A. J. Ferguson, D. Zhao, K. Wijeratne, A. Würger, J. L. Blackburn, X. Crispin and S. Fabiano, *Chem. Rev.*, 2021, **121**, 12465–12547.
26 S. Wang, J. Wu, F. Yang, H. Xin, L. Wang and C. Gao, *ACS Appl. Mater. Interfaces*, 2021, **13**, 26482–26489.
27 S. Horike, T. Fukushima, T. Saito, T. Kuchimura, Y. Koshiba, M. Morimoto and K. Ishida, *Mol. Syst. Des. Eng.*, 2017, **2**, 616–623.
28 M. Wong, M. Paramsothy, X. Xu, Y. Ren, S. Li and K. Liao, *Polymer*, 2003, **44**, 7757–7764.
29 S. Hata, M. Kusada, S. Yasuda, Y. Du, Y. Shiraishi and N. Toshima, *Appl. Phys. Lett.*, 2021, **118**, 243904.
30 R. Dong and J. Hao, *Chem. Rev.*, 2010, **110**, 4978–5022.
31 L.-J. Chen, S.-Y. Lin, C.-C. Huang and E.-M. Chen, *Colloids Surf., A*, 1998, **135**, 175–181.
32 E. Bekyarova, M. E. Itkis, N. Cabrera, B. Zhao, A. Yu, J. Gao and R. C. Haddon, *J. Am. Chem. Soc.*, 2005, **127**, 5990–5995.
33 J. W. Jo, J. W. Jung, J. U. Lee and W. H. Jo, *ACS Nano*, 2010, **4**, 5382–5388.
34 S. Hata, M. Shiraishi, S. Yasuda, G. Juhasz, Y. Du, Y. Shiraishi and N. Toshima, *Energy Mater. Adv.*, 2022, 9854657.
35 T. Fukumaru, T. Fujigaya and N. Nakashima, *Sci. Rep.*, 2015, **5**, 7951.
36 S. L. Kim, K. Choi, A. Tazebay and C. Yu, *ACS Nano*, 2014, **8**, 2377–2386.
37 C. Yu, A. Murali, K. Choi and Y. Ryu, *Energy Environ. Sci.*, 2012, **5**, 9481.
38 W. Zhou, Q. Fan, Q. Zhang, L. Cai, K. Li, X. Gu, F. Yang, N. Zhang, Y. Wang, H. Liu, Z. Weiya and X. Sishen, *Nat. Commun.*, 2017, **8**, 14886.
39 X. Cheng, X. Wang and G. Chen, *J. Mater. Chem. A*, 2018, **6**, 19030–19037.
40 Y. Liu, Q. Dai, Y. Zhou, B. Li, X. Mao, C. Gao, Y. Gao, C. Pan, Q. Jiang and Y. Wu, *ACS Appl. Mater. Interfaces*, 2019, **11**, 29320–29329.
41 S. Horike, Q. Wei, K. Kirihara and M. Mukaida, *Chem. Phys. Lett.*, 2020, **755**, 137801.
42 X. Nie, X. Mao, X. Li, J. Wu, Y. Liu, B. Li, L. Xiang, C. Gao, Y. Xie and L. Wang, *Chem. Eng. J.*, 2021, **421**, 129718.
43 S. Horike, Q. Wei, K. Akaike, K. Kirihara, M. Mukaida, Y. Koshiba and K. Ishida, *Nat. Commun.*, 2022, **13**, 3517.
44 Y. Wang, Q. Li, J. Wang, Z. Li, K. Li, X. Dai, J. Pan and H. Wang, *Nano Energy*, 2022, **93**, 106804.
45 T. Sakakura, J.-C. Choi and H. Yasuda, *Chem. Rev.*, 2007, **107**, 2365–2387.
46 R. A. Pramudita, K. Nakao, C. Nakagawa, R. Wang, T. Mochizuki, H. Takato, Y. Manaka and K. Motokura, *Energy Adv.*, 2022, **1**, 385–390.